2020 11th International Conference on Electrical and Computer Engineering (ICECE)

S-Parameters Based Channel Characterization Using Ultra-Wideband Pulse Signal

Md. Kamal Hossain* and Mohammad R. Haider*
*School of Engineering, University of Alabama at Birmingham, Birmingham, AL, USA

2020 11th International Conference on Electrical and Computer Engineering (ICECE) | 978-1-6654-2254-3/20/$31.00 ©2020 IEEE | DOI: 10.1109/ICECE51571.2020.9393063

***Abstract*—Ultra-Wideband has recently become a powerful technology that involves wireless communication, digital signal processing, machine learning, and even hardware design for ubiquitous sensing applications. This paper presents a straight forward signal processing method to characterize the wireless communication channel using the UWB pulse signal. This proposed method uses a narrow width based modified Hermitian pulse (MHP) for calculating the output signal at the receiver end from measured network parameters. Magnitude attenuation, wave shape distortion, and phase shift of the output signal indicate the impact of the communication channel on the traveling wave. A neural network-based deep learning algorithm uses to classify the obstacle types from the measured output signal using the MATLAB tool. Measurement results demonstrate the real scenario of channel effects on the high-frequency UWB signal and select a suitable modulation scheme for data encoding. It also helps design the receiver compensation, reconstruct the distorted signal, and channel access to use the MHP pulse signal for high-density data communication. This method can also be used other sensing applications such as damage localization, detection, displacement measurement, material identification, etc.**

***Index Terms*—S-parameters, orthogonal pulse, composite pulse, communication systems, and signal processing.**

I. Introduction

Ultra-Wideband (UWB) technology has become a feasible and robust wireless data communication system in a wireless sensor network (WSN). The pulse-based UWB system is based on sub-nanosecond pulses with carrier or without carrier signal to transmit information from sensor nodes to the data center. Typically, UWB system modulates the sensor data by a narrow width pulse, and low power over a spectrum of frequencies ranging from 3.1 GHz to 10.5 GHz. Therefore, UWB technology is entirely health-risk free for wireless data communication in sensor networks. Due to the unique characteristics of UWB signals such as higher penetration capabilities, extremely precise ranging, resource constraint applications, low cost, simple hardware, and robustness to multi-path interference's, UWB technology is widely used for non-invasive medical applications, localization, ubiquitous sensing, high-speed data communications, etc [1]–[3].

Many research articles have studied using short duration pulse signals to transmit high-speed data for WSN applications to extend the target detection and optimize Radar waveform design. Recently, a multi-order UWB pulse-based data encoding scheme has been proposed to transmit a large volume of the sensor by supporting multi-channel data within existing bandwidth [4], [5]. A UWB based Radar sensor has been investigated to detect the object behind obstacles to search and rescue human security. A perfect and straightforward human detection approach based on standard deviation has proposed [2] to avoid computational load in a discrete Fourier transform. An innovative WSN based on UWB technology has developed for landslide monitoring of ground deformation where the available resources are inadequate [3]. The UWB based sensing system for detecting human vital sign signals such as respiration and heart rates behind the obstacles has been proposed by estimating the phase variations of received respiration frequency [6]. A machine learning (ML) based image processing technique has proposed recognizing digits written by hand moving through air media using multiple UWB Radar sensors [7], [8]. However, tremendous R & D efforts are required to develop the UWB system, including channel characterization, transceiver design, coexistence, with other narrowband system, etc.

Typically, the conventional pulse-based UWB system uses the narrow-width pulse for data communication and sensing applications. Different pulse generation schemes are available, such as Gaussian pulse, Haar function, Hermitian polynomial, etc [9], [10]. However, the existing pulse generation scheme suffers from system complexity, computational speed, power consumption, etc. A pulse duration of 540 ps signal generation scheme is developed using FPGA for human detection through obstacle [9]. A power-efficient and simple architecture-based multi-order analog pulse generation scheme has developed for the UWB system [11]. The MHP set has signal orthogonality, coexist with other applications, and suitable for wireless communication. Therefore, to simplify the transceiver architecture, an efficient pulse generation scheme requires low power sensor applications. In this paper, an orthogonal MHPs based UWB sensor using the ML technique is proposed to detect an obstacle in communication channels.

This paper proposes a straightforward signal processing method using time-frequency analysis to detect the obstacles when passing through it. This work is motivated by the scattering parameter measurements using a bench-top vector network analyzer (VNA) to recover the time-domain ultrasound signal from the frequency-domain [12]. This proposed method aims to classify the obstacle types based on their receiving time-domain signal pattern using machine learning algorithms. The rest of this paper is organized as

follows: Section II and section III represents the background study on S-parameter based sensing method and test setup, measurements, and computation. Section IV describes the results and finally concludes the paper in section V.

II. S-Parameters Based Sensing Method

The electromagnetic (EM) response of a signal depends on the permittivity of the propagation media. Moreover, the high-frequency time-varying signal's amplitude and phase are distorted when traveling through a linear circuit. Therefore, the accurate measurement of the permittivity and frequency-response of the time-varying signal is crucial for sensing and detection applications. In the non-resonant measurement approach, the material permittivity is calculated from the changes of the characteristics impedance and wave velocity of EM by the reflection and transmission coefficient. In the non-resonant measurement approach, the EM wave directs towards a device under test (DUT) and collects the reflected and transmitted signal traveling through devices [13].

A. Background on Two-port Network

S-parameters are mostly used for electrical networks and operated at radio and microwave frequencies to describe amplitude and phase distortion of a time-varying signal traveling through a linear network or media. Fig. 1 shows the electrical two-port network diagram for representing the S-parameters. The signal reflection and transmission coefficients at port 1 and port 2 represents by S_{11}, S_{22}, S_{21}, and S_{12} parameters. In this diagram, 'X_1' & 'X_2' are two input signals at ports 1 & 2 and 'Y_1' & 'Y_2' are the corresponding reflected signals respectively. If we assume that each port is terminated in the reference impedance Z_o, then the four S-parameters can be defined as a matrix algebraic representation. Typically, S-parameters are the complex function and expressed in the frequency domain.

$$\begin{pmatrix} Y_1 \\ Y_2 \end{pmatrix} = \begin{pmatrix} S_{11} & S_{12} \\ S_{21} & S_{22} \end{pmatrix} * \begin{pmatrix} X_1 \\ X_2 \end{pmatrix}$$

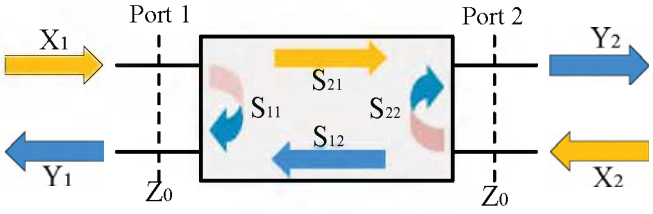

Fig. 1. S-parameter representation of a two-port network.

B. S-Parameter Based Computation Approach

In signal processing, an electrical signal can be represented by both in the time-domain and frequency-domain. Though the signal shows different properties in their representation; however, these representations are equivalent and contains all the information to characterize them fully. Moreover, a signal can be translated from time-domain (TD) to frequency-domain (FD) via Fourier transform and back again in TD from FD by inverse Fourier transform without losing any information. Fig. 2 shows the signal conversion approach and measure in the TD signal from S-parameters measurements. Let, X(t) in TD is the network input signal at the transmitter. The frequency spectrum, X(ω) of the input signal, can be calculated using a fast Fourier transform (FFT). The output Y(ω) signal at the receiver end traveling through the communication channel can be calculated by multiplying with the power transmission coefficient $S_{21}(\omega)$ from TX to RX. The TD signal can be extracted from the FD signal at the receiver by applying the inverse FFT to (3). The desire output results at the receiver can be obtained through digital signal processing (DSP) computation from equation (1) to (3) and implemented signal recognition algorithm.

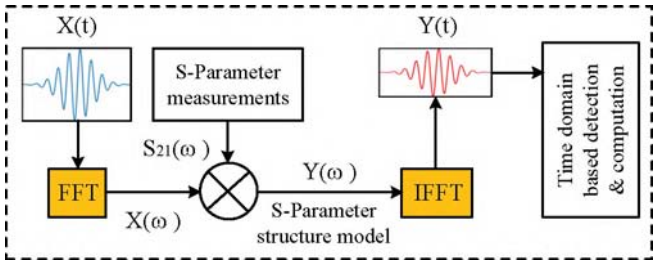

Fig. 2. The functional block diagram for S-parameter based sensing approach.

$$X(\omega) = FFT[X(t)] \tag{1}$$

$$Y(\omega) = S_{21}(\omega) * X(\omega) \tag{2}$$

$$Y(t) = IFFT[Y(\omega)] = IFFT[S21(\omega) * X(\omega)] \tag{3}$$

III. Test Setup, Measurements and Computation

This section presents the MHP pulse signal generation scheme, test set-up for S-parameter measurements using a VNA, and signal processing using MATLAB Simulation tools. A short description of each subsection as follows:

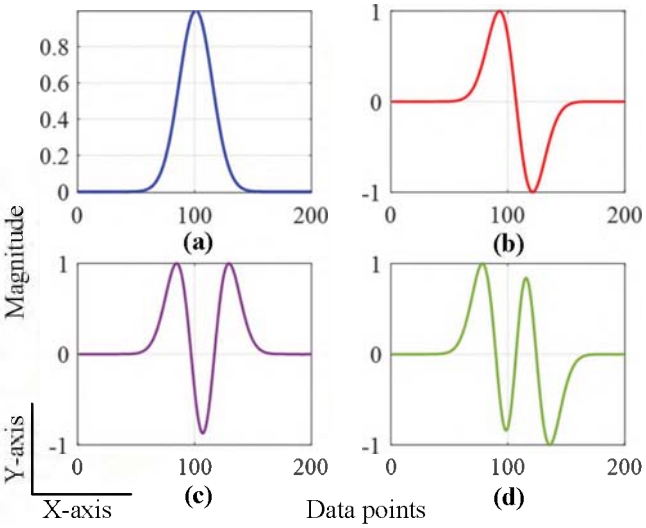

Fig. 3. Orthogonal MHPs (a) MHP0, (b) MHP1, (b) MHP2, and (c) MHP3.

A. Orthogonal MHPs Set Generation

In this work, we use the multi-order orthogonal pulse set generator describes in [11]. This power-efficient and straightforward orthogonal pulse generation scheme consists of two first-order Hermitian polynomials that improve computational simplicity. It was designed for the sub-GHz frequency band for pulse-based UWB communications with a pulse width of 20 ns. The higher-order orthogonal pulse is generated by changing the value of n from zero to any finite number. This work uses the composite pulse signal consisting of the first four distinct zeroth, first, second, and third orders orthogonal pulses represents by MHP0, MHP1, MHP2, and MHP3, respectively, to observe the effects on time-varying MHPs traveling through channel obstacles.

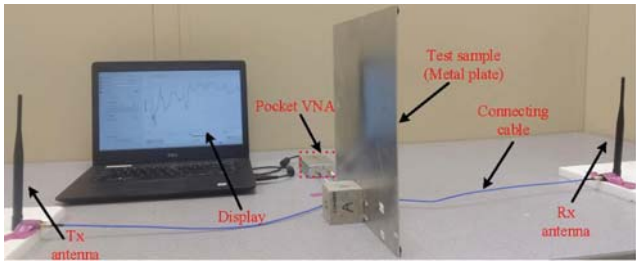

Fig. 4. S-parameter measurements setup using a pocket VNA.

B. Vector Network Analyzers

In this work, the S-parameters are measured by a portable 2-port VNA known as Pocket VNA. This portable VNA can measure DUT's frequency response up to 4.0 GHz, and display measurements result in laptop or desktop computer screen via user interface software. Fig. 4 shows the S-parameters test set-up of measuring network parameters using a typical pocket VNA. Usually, a VNA measures the S-parameters of a DUT by directly measuring the components such as magnitude and phase variation of the signal with changing the range of frequencies or a single frequency. The VNA is calibrated using the standard calibration kits before measuring the S-parameters of the sample. In this work, the TX and RX antenna is placed in 4.0 feet distance and connect with pocket VNA via the calibrated co-axial cable. To initiate devices' and characterize the communication channel a test sample DUT (i.e metal, wood, and foam) places in the middle of TX and RX antenna. The built-in source of VNA provides a stimulus signal injects into DUT and measures the frequency response. It derives the reflection and transmission signals by measuring the magnitude and phase by sweeping the frequencies in interest range. Once the measurement is done, the VNA calculates S-parameters according to the two-ports network's expression and displays the results.

C. Signal Processing and Time Domain Signal Calculation

In this paper, we create a composite pulse signal 5(a) using orthogonal MHP0, MHP1, MHP2, and MHP3 pulses to observe the signal distortion after penetrating through different media such as free space, foam, metal, and wooden blockage. The low-frequency composite pulse signal modulates with

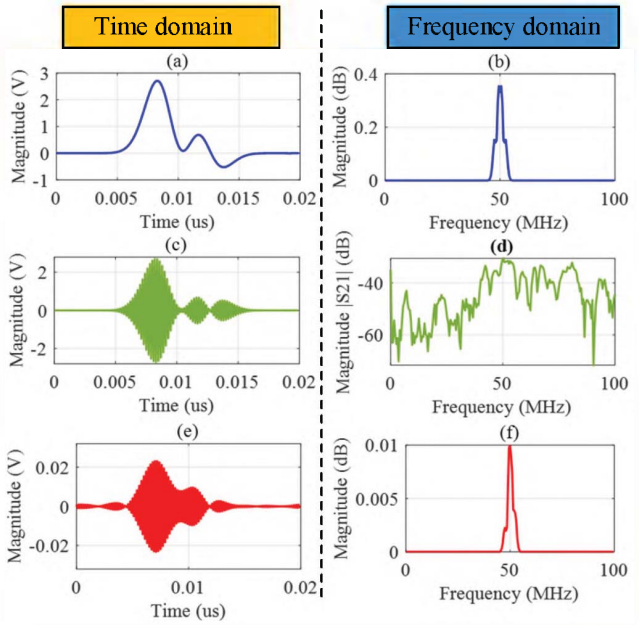

Fig. 5. Time domain signal generation from s-parameter measurements.

a carrier to translate the signal frequency for long-distance propagation. Fig. 5(b) represents the amplitude modulated signal with a sinusoidal carrier at 500 MHz. In signal processing computation, the TD input signal converts to FD using FFT. Fig. 5(d) and (e) presents the input signal $X(\omega)$ and the measured $S_{21}(\omega)$ signal. Fig. 5(f) represents the output signal calculated from input $X(\omega)$ and S-parameters $S_{21}(\omega)$ signal. Finally, to extract the time-varying output Y(t) uses the IFFT of resultants S-domain signal, $Y_(\omega)$. Fig. 5(e) depicts the time-domain output signal with the carrier frequency. To recover the baseband signal demodulates the output signal by the same carrier frequency. The channel blockage detects by observing the signal distortion/wave shape change from the measured time-varying output. The ML technique uses to detect the obstacle types using the previously trained data set.

IV. Results and Discussion

The S-parameter measurements are taken in different cases by placing the channel blockage between TX and RX antenna. The S_{21} is measured by sweeping the frequencies from 100 kHz to 1.0 GHz with 200 steps. In all cases, the measured S_{21} spectra are used to calculate the time-varying output signal through signal processing process describes in III-C. The time-frequency signal analysis is performed using MATLAB 2019(a) simulation package. Fig. 6 (a), (b), (c), and (d) shows the time-varying waveforms generated from S_{21} measurement at free-space, foam blockage, metal blockage, and wooden blockage, respectively. The signal distortion of output signal, represents the obstacle properties and characterize the communication channel.

In Fig. 6 depicts that, the output signal at RX is identical in all cases with some variations from one signal to another. Typically, signal distortion depends on the material properties, types, area, frequency, etc. In this works, the line-of-sight propagation is considered to observe the signal properties

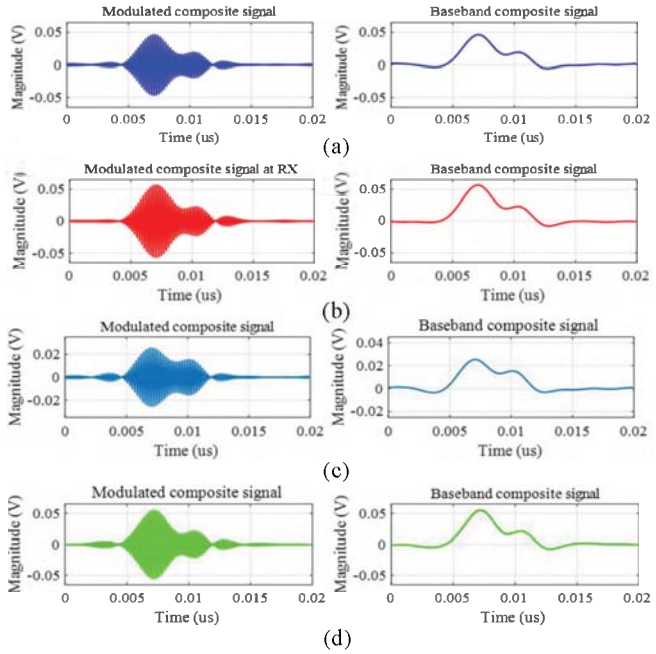

Fig. 6. Output signal calculated from measured S-parameters.

after penetrating through obstacle in communication channel. The dielectric constant of foam is close to free-space (1.0), aluminum sheet (4.5), and dry wood (2.0 to 6.0) that causes the signal distortion when traveling through it. Therefore, the output signal for free-space and foam blockage is almost same (Fig. 6 (a) & (b)). However, the measured time-varying signal for metal and wood is distorted more compared to foam and air (Fig. 6 (c) & (d)) due to higher dielectric constant.

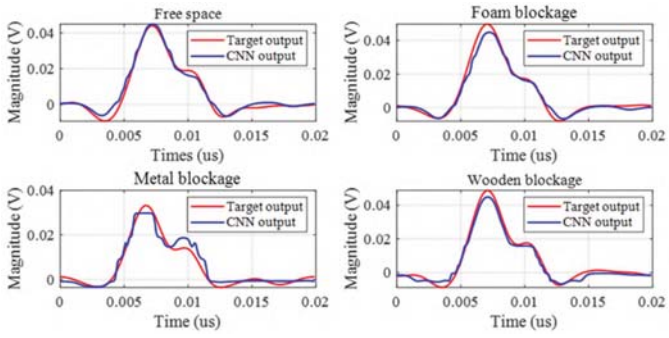

Fig. 7. Time varying output signal tracking using neural network.

This work uses a convolutional neural network (CNN) to detect and classify the obstacle types in the communication path using MATLAB nntool. Fig. 7 shows the CNN test results of output signal tracking using an ML algorithm. In this test, 4-neural network is trained separately by multiple test data of each case's time-varying output signal. Typically, in the same sample, the S-parameter measurement results vary due to environmental effect (without anechoic chamber), changing of obstacles position, other reflection effects etc. Therefore, the time-varying output signal also changes with measured S-parameters. For accurate signal tracking, each network is trained by 8-different test data set and select one as a target output in four cases. Then the network is tested by another output data set of measured time-varying signal and checked the CNN results. In Fig. 7, the solid blue and dotted red trace indicate the measured and target wave shape of the output signal using the CNN test. The measured signal is tracked correctly, the target output signal for each sample. Therefore, the ML computation simplifies the time-varying output signal detection process and classify the obstacles accurately.

V. Conclusion

A straightforward signal processing method is presented in this paper to measure the time-domain signal based on S-parameters measurement. The composite pulse signal is generated using a power-efficient pulse set generator to characterize the communication channel for high-density data transmission using MHP pulses. The measurement results indicate that the proposed methods can detect the communication channel's impact on the time-varying signal when traveling through it. The test results also differentiate the channel blockage types and modify transceiver architecture for decoding the individual pulses from composite signals. It also suggests a proper modulation scheme and signals compensator design to reconstruct the original composite signal from received distorted signal for MHP pulse-based wireless data transmission. It also can be used to detect, localize, damage identification, and other sensing applications.

Acknowledgment

This work was supported by the NSF under the Award no. ECCS-1813949 and CNS-1645863.

References

[1] M. Chiani, A. Giorgetti, and E. Paolini, "Sensor Radar for Object Tracking," in Proceedings of the IEEE, vol. 106(6), pp. 1022-1041, 2018.
[2] S. D. Liang, "Sense-through-wall human detection based on UWB radar sensors," Signal Processing, vol. 126, pp. 117-124, 2016.
[3] M.Lorenzo et al., A Flexible Wireless Sensor Network Based on Ultra-Wide Band Technology for Ground Instability Monitoring, Sensors (Basel, Switzerland), vol. 18(9):2948. 5 Sep. 2018.
[4] M. K. Hossain, Y. Massoud and M. R. Haider, "A Spectrum-Efficient Data Modulation Scheme for Internet-of-Things Applications," 2020 IEEE 63rd International Midwest Symposium on Circuits and Systems, Springfield, MA, USA, 2020, pp. 770-773.
[5] M. K. Hossain, M. I. Rashid, M. R. Haider and M. T. Rahman, "Randomized Pulse-Based Encoding for Secure Wireless Data Communications," 2020 IEEE 63rd International Midwest Symposium on Circuits and Systems, Springfield, MA, USA, 2020, pp. 289-292.
[6] X. Liang, H. Zhang, G. Fang, S. Ye and T. A. Gulliver, "An Improved Algorithm for Through-Wall Target Detection Using Ultra-Wideband Impulse Radar," in IEEE Access, vol. 5, pp. 22101-22118, 2017.
[7] S. K. Leem, F. Khan and S. H. Cho, "Detecting Mid-Air Gestures for Digit Writing With Radio Sensors and a CNN," in IEEE Transactions on Instrumentation and Measurement, vol. 69, no. 4, pp. 1066-1081, 2020.
[8] L. Jiao, et. all, "A survey of deep learning-based object detection", IEEE Access, vol. 7, pp.128837-128868, 2019.
[9] L. Tantiparimongkol, et. all, "IR-UWB Pulse Generation Using FPGA Scheme for through Obstacle Detection", Sensors, vol. 20(3750), 2020.
[10] H. Werfelli, et. all, "Design of a pulse generator for UWB communications," 10th International Multi-Conferences on Systems, Signals and Devices 2013 (SSD13), Hammamet, 2013, pp. 1-6.
[11] Y. Li, et. all, "An efficient orthogonal pulse set generator for high speed sub-GHz UWB communications," 2014 IEEE International Symposium on Circuits and Systems (ISCAS), Melbourne VIC, 2014, pp. 1913-1916.
[12] H. Huang, et. all, "Introducing S-parameters for ultrasound-based structural health monitoring", in IEEE Transactions on Ultrasonics, Ferroelectrics, and Frequency Control, vol. 61(11), pp.1856-1863.
[13] J. Yeo, and J.I. Lee, "High-sensitivity microwave sensor based on an interdigital-capacitor-shaped defected ground structure for permittivity characterization", in Sensors, vol. 19(3), pp.498, 2019.